

Piezoelectrics by Design: A Route through Short-period Perovskite Superlattices

Hena Das¹, Umesh V. Waghmare², T. Saha-Dasgupta¹

¹ Department of Materials Science, S.N. Bose National Centre for Basic Sciences, Kolkata 700098, INDIA

² Jawaharlal Nehru Centre for Advanced Scientific Research, Jakkur, Bangalore-560 064, India

(Dated: May 25, 2022)

Using first-principles density functional theory, we study piezoelectricity in short-period superlattices made with combination of ferroelectric and paraelectric components and exhibiting polar discontinuities. We show that piezoelectric response of such a superlattice can be tuned both in terms of sign and magnitude with a choice of its components. As these superlattices with non-switchable polarization do not undergo ferroelectric transitions, we predict them to exhibit a robust piezoelectric response with weaker temperature dependence compared to their bulk counterparts.

PACS numbers: 73.20.-r, 77.84.-s, 71.15.Nc

With advances in experimental techniques, it is now possible to create superlattices of various of oxide perovskites (general formula ABO_3) through layer by layer epitaxial growth. Such superlattices have attracted lot of attention in recent years due to the presence of unusual properties.¹⁻⁷ In particular, these superlattices may exhibit polar discontinuities leading to the so-called "polar catastrophe", a topic of much discussion in recent time in the context of $LaAlO_3/SrTiO_3$ thin films.^{2-5,8}

Superlattices with polar discontinuity were studied by Murray and Vanderbilt⁹ from first-principles for superlattices consisting of ferroelectric (FE) and paraelectric (PE) components, and the "polar catastrophe" was found to result in response of system in terms of polar distortions at the interface. This was extended in our recent work¹⁰ to superlattices with ultra-thin (1 unit-cell) components of FE and PE layers. Our study¹⁰ carried out on a series of such superlattices constructed from different PE and FE components showed that even for ultra-thin superlattices, systems containing polar discontinuities have strongly broken inversion symmetry and large non-switchable polarization. The magnitudes of the polar distortions are as large as those in the corresponding bulk FE materials. Evidently, this class of superlattices form promising new material with interesting properties.

In a recent study, tunability of piezoelectric properties of short period ferroelectric superlattices with strain was investigated.¹¹ Here we demonstrate tunability of robust piezoelectric properties for superlattices formed of FE and PE layers through (i) polar discontinuity and (ii) chemical control, using first-principles density functional theory (DFT) based calculations.

We consider two representative systems: $LaAlO_3/PbTiO_3$ (LAO/PTO) and $KSbO_3/PbTiO_3$ (KSO/PTO) and design composite superlattices formed out of these two superlattices, such as $KSbO_3/PbTiO_3/LaAlO_3/PbTiO_3$ (KSO/PTO/LAO/PTO). The first two systems are composed of alternating III-III ($A^{+3}B^{+3}O_3$)/II-IV ($A^{+2}B^{+4}O_3$) and I-V ($A^{+1}B^{+5}O_3$)/II-IV perovskite layers respectively, while the last system is composed of alternating I-V/II-IV/III-III/II-IV sequence.

Our calculations are carried out in the plane wave

basis within the framework of local density approximation (LDA) of DFT using the Vienna Ab-initio simulation package (VASP).¹²⁻¹³ The positions of the ions are relaxed towards equilibrium until the Hellmann-Feynman forces become less than $0.001 \text{ eV}/\text{\AA}$. A $6 \times 6 \times 4$ Monkhorst-Pack k-point mesh and 450 eV plane-wave cut off are used for the calculations. The polarization is calculated using the Berry phase approach¹⁴ of modern theory of polarization. To determine piezoelectric response, strains of $\pm 1\%$ are applied. The superlattices are constructed along the crystallographic z direction, and the piezoelectric coefficient relevant to applications is e_{zz} , strain is therefore applied along the z direction.

Fig.1 shows equilibrium geometries obtained by relaxation of the atomic positions and the out of plane lattice constants (c), with the in-plane lattice constant (a) fixed to the LDA bulk lattice constant of $PbTiO_3$ in the tetragonal phase. The presence of polar discontinuities drive both LAO/PTO and KSO/PTO strongly polar, as found in Ref¹⁰. The opposite orientation of the polar discontinuity in case of LAO/PTO and KSO/PTO gives rise to off-centric movements of Pb and Ti that are oppositely oriented in two cases. The off-centric movements driven entirely by the polar discontinuity are non-switchable. The third superlattice built up with combination of LAO/PTO and KSO/PTO superlattices, impose oppositely directed polar fields on the PTO layer, as shown in Fig.1. This leads to the interesting situation, where the off-centric movements of Pb and Ti ions become negligibly small and the cations in the PE layers move significantly with the movements of La and Al being opposite in direction to that of K and Sb. The off-centric movements of La, Al, K and Sb measured with respect to the centers of their oxygen cages are found to be as large as 0.25 \AA , 0.16 \AA , -0.21 \AA and -0.17 \AA respectively. This may be compared with the large displacements of Pb and Ti in case of LAO/PTO and KSO/PTO, which are found to be -0.25 \AA and -0.15 \AA respectively for LAO/PTO and 0.29 \AA and 0.18 \AA respectively for KSO/PTO. This gives rise to a calculated polarization value of $12.79 \mu C/cm^2$ compared to $-50.87 \mu C/cm^2$ for LAO/PTO, $+57.74 \mu C/cm^2$ for KSO/PTO, reduced by a factor of 4 - 4.5 in composite superlattice compared to

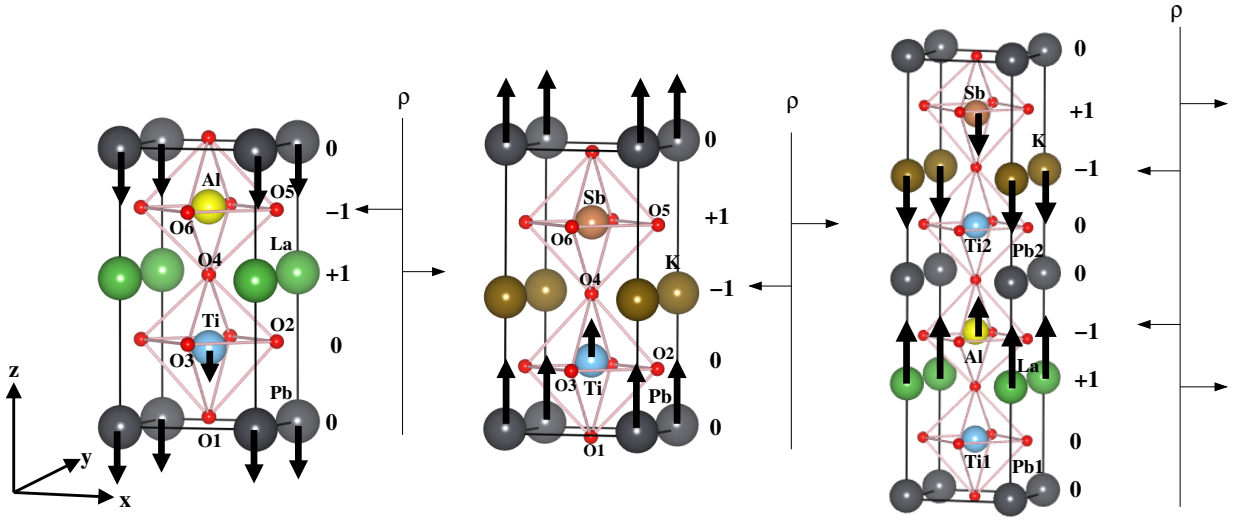


FIG. 1: (Color Online) Equilibrium structures of LAO/PTO, KTO/PTO and the composite superlattice KAO/PTO/LAO/PTO (from left to right). The arrows mark the various off-centric movements of the cations measured from the centers of their respective oxygen cages. For clarity, only the off-centric movements larger than 0.05 \AA are shown. The polar discontinuities arising in each superlattices are shown in terms of formal charges (ρ).

its components.

To determine piezoelectric coefficients of the constructed superlattices, in the next step we calculate polarization at unstrained structure (P^{ref}) and at several strained structures (P^ϵ), with relaxed atomic positions. The slope of the ($P^\epsilon - P^{ref}$) versus strain curve yields the piezoelectric constants, e_{zz} . Fig. 2 shows such curves for LAO/PTO, KSO/PTO and KSO/PTO/LAO/PTO superlattices. We find the piezoelectric coefficient to be large and negative (-2.58) for LAO/PTO, large and positive ($+4.08$) for KSO/PTO and a small value (0.48) for KSO/PTO/LAO/PTO. Using combination of various perovskite materials, we are therefore able to design piezoelectrics with e_{zz} of opposite sign and varied magnitudes.

To have large piezoelectric effect, the system must contain ions with large Born effective charges (Z^*) and they should easily move as a result of lattice strain. A piezoelectric coefficient can be separated into two parts: a clamped-ion contribution evaluated at vanishing values of the movements of the ions (u), and a term that is due to the displacements of differently charge sublattices¹⁵:

$$e_{zz} = \left. \frac{\partial P_z}{\partial \epsilon_{zz}} \right|_{u=0} + \sum_k \frac{\partial P_z}{\partial u_k} \frac{\partial u_k}{\partial \epsilon_{zz}} = e^0 + \sum_k \frac{q_e}{\Omega} Z^* \frac{\partial u_k}{\partial \epsilon_{zz}} \quad (1)$$

where Ω is the volume, q_e is the electronic charge and the subscript k corresponds to the atomic sublattices. Table -I lists the various contributions for LAO/PTO, KSO/PTO and KSO/PTO/LAO/PTO superlattices. We find large sensitivity of atomic movements upon strain for Pb, O1 (oxygen at Pb plane) for LAO/PTO system, for Pb, Ti, O1 (oxygen at Pb plane), O5/O6 (oxygens at the Sb plane) for KSO/PTO sys-

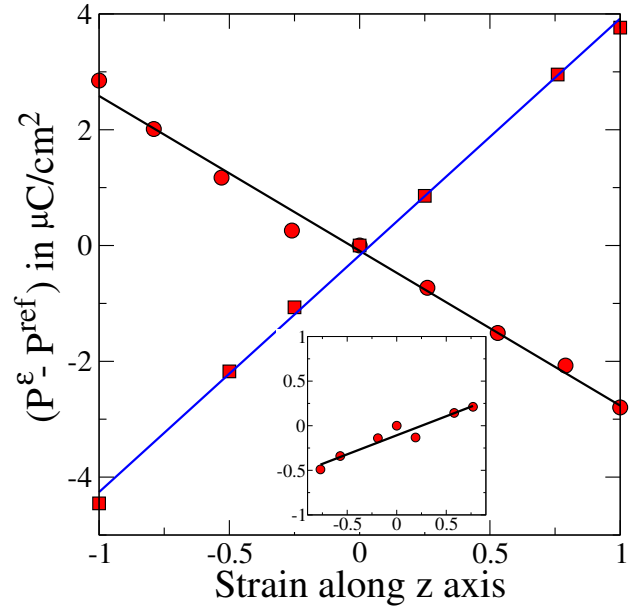


FIG. 2: ($P^\epsilon - P^{ref}$) for LAO/PTO (circles) and KSO/PTO (squares) plotted as function of applied strain along z direction. Inset shows the same plot for KAO/PTO/LAO/PTO. The slope of each curve give the measure of piezoelectric coefficient (see text). Note the change in y -scale between the inset and the main plot.

tem. The composite system on the other hand, is far more rigid, with $\partial u/\partial \epsilon$ values being order of magnitude smaller. Born effective charges, however, change only slightly between the composite superlattice and the

TABLE I: Internal displacement gradients as a function of strain ($\partial u_{k,z}/\partial \epsilon_z$), Born effective charges (Z_{zz}^*) for different ions in LAO/PTO and KSO/PTO superlattices. The numbers in the bracket indicate the corresponding numbers for the composite superlattice KSO/PTO/LAO/PTO. Clamped ion contribution to total piezoelectric coefficient (e^0), contribution due to internal microscopic strain (e^1), the total contribution $e^0 + e^1$ ($e_{zz}^{indirect}$) and the piezoelectric coefficient obtained from the slopes in Fig.2 (e_{zz}^{direct}) are also listed.

LAO/PTO				KSO/PTO			
k	$\frac{\partial u_{k,z}}{\partial \epsilon_z}$	Z_{zz}^*	$Z_{zz}^* * \frac{\partial u_{k,z}}{\partial \epsilon_z}$	k	$\frac{\partial u_{k,z}}{\partial \epsilon_z}$	Z_{zz}^*	$Z_{zz}^* * \frac{\partial u_{k,z}}{\partial \epsilon_z}$
Pb	-0.15 (0.03)	3.42 (3.05)	-0.51 (0.08)	Pb	0.14 (0.03)	2.88 (3.08)	0.40 (0.09)
La	-0.06 (0.00)	4.71 (3.70)	-0.28 (0.00)	K	0.10 (0.02)	1.23 (1.35)	0.12 (0.03)
Ti	-0.08 (0.02)	5.56 (4.82)	-0.44 (0.08)	Ti	0.15 (-0.02)	5.38 (5.52)	0.80 (-0.13)
Al	-0.04 (-0.06)	3.69 (3.63)	-0.14 (-0.20)	Sb	0.12 (0.05)	6.04 (5.85)	0.72 (0.31)
O1	0.13 (0.05)	-3.73 (-3.39)	-0.48 (-0.18)	O1	-0.14 (-0.03)	-3.11 (-3.43)	0.44 (0.11)
O2/O3	0.09 (0.00)	-2.11 (-1.74)	-0.19 (0.00)	O2/O3	-0.09 (-0.02)	-1.61 (-1.68)	0.15 (0.04)
O4	0.04 (0.06)	-3.58 (-3.36)	-0.14 (-0.18)	O4	-0.06 (-0.03)	-4.99 (-4.69)	0.30 (0.15)
O5/O6	0.07 (-0.02)	-2.96 (-2.57)	-0.20 (0.06)	O5	-0.17 (-0.01)	-2.07 (-2.13)	0.35 (0.02)
e^0 (C/m ²)	e^1 (C/m ²)	$e_{zz}^{indirect}$ (C/m ²)	e_{zz}^{direct} (C/m ²)	e^0 (C/m ²)	e^1 (C/m ²)	$e_{zz}^{indirect}$ (C/m ²)	e_{zz}^{direct} (C/m ²)
0.17	-3.01	-2.85	-2.58	-0.10 (0.07)	4.09 (0.41)	3.99 (0.45)	4.08 (0.48)

TABLE II: The phonon modes that contribute significantly (in the table the percentage contribution is denoted by C) in the piezoelectric response. Frequencies are listed for the equilibrium geometry and that under +1% and -1% strain.

	LAO/PTO				KSO/PTO		
	ω in cm ⁻¹				ω in cm ⁻¹		
C	-1%	0	+1%	C	-1%	0	+1%
17	371.73	363.04	352.41	10	286.24	284.69	268.81
10	317.19	302.56	295.93	29	210.94	209.94	212.97
28	185.79	181.18	179.51	24	200.61	194.37	196.99
35	116.57	115.19	110.25	28	117.44	125.83	115.37

individual superlattices, with the exception of La and O2/O3.

Due to non-switchable polarization, it is expected that these superlattices would exhibit piezoelectric properties that show weaker temperature dependence than the conventional, bulk piezoelectric materials like PbTiO₃. To explore this, we determine Γ -point phonons for the superlattices exhibiting strong piezoelectric responses, i.e LAO/PTO and KSO/PTO, and decompose the displacements of the ions upon strain in terms of these nor-

mal modes. Table II lists the frequencies of phonon modes that dominantly contribute to the piezoelectric coefficients and their changes upon +1% and -1% lattice strain. The frequencies are found to change by 1-4%, except for the softest ones for which the change about 6-8%. This is in contrast to larger (14%) change in the soft mode ($\omega = 141$ cm⁻¹) of tetragonal PbTiO₃ with 1% strain, which is known to cause strong temperature dependence in its piezo and dielectric responses. With relatively smaller Grüneisen parameter, these superlattices, therefore, should have a piezoelectric response that is relatively robust as a function of temperature.

In conclusion, we presented the analysis of piezoelectric properties of bi-component, ultra-thin superlattices processing polar discontinuities. We demonstrated tunability of their piezoelectric response via appropriate choice of different components, providing a chemical control. Moreover their piezoelectric properties are expected to be only weakly temperature dependent compared to conventional piezoelectrics, opening up a new avenue for piezoelectrics by design.

UVW thanks IBM faculty award and DST for funding. TSD acknowledges support from DST through AMRU project.

¹ A. Ohtomo, D. A. Muller, J. L. Grazul, H. Y. Hwang, Nature **419**, 378 (2002).

² A. Ohtomo and H. Y. Hwang, Nature (London) **427**, 423 (2004).

³ A. Brinkman, M. Huijben, M. van Zalk, J. Huijben, U. Zeitler, J. C. Maan, W. G. van der Wiel, G. Rijnders, D. H. A. Blank, and H. Hilgenkamp, Nature Mater. **6**, 493 (2007).

⁴ N. Reyren, S. Thiel, A. D. Caviglia, L. Fitting Kourkoutis,

G. Hammerl, C. Richter, C. W. Schneider, T. Kopp, A.-S. Retschi, D. Jaccard, M. Gabay, D. A. Muller, J.-M. Triscone, and J. Mannhart, Science **317**, 1196 (2007).

⁵ A. D. Caviglia, S. Gariglio, N. Reyren, D. Jaccard, T. Schneider, M. Gabay, S. Thiel, G. Hammerl, J. Mannhart, and J.-M. Triscone, Nature (London) **456**, 624 (2008).

⁶ Serban Smadici, Peter Abbamonte, Anand Bhattacharya, Xiaofang Zhai, Bin Jiang, Andrivo Rusydi, James N. Eckstein, Samuel D. Bader, and Jian-Min Zuo, Phys. Rev.

- Lett. **99**, 196404 (2007).
- ⁷ Phillippe Ghosez et al., *Nature Mat.* **452**, 732 (2008).
- ⁸ N. Nakagawa, H. Y. Hwang, and D. A. Muller, *Nature Mater.* **5**, 204 (2006).
- ⁹ E. Murray and D. Vanderbilt, *Phys. Rev. B* **79**, 100102 (2009).
- ¹⁰ H. Das, N. A. Spaldin, U. V. Waghmare, and T. Saha-Dasgupta, *Phys. Rev. B* **81**, 1 (2010).
- ¹¹ V. R. Cooper and K. M. Rabe, arXiv:0901.0896v2.
- ¹² G. Kresse and J. Hafner, *Phys. Rev. B* **47**, R558 (1993).
- ¹³ G. Kresse and J. Furthmuller, *Phys. Rev. B* **54**, 11169 (1996).
- ¹⁴ R. D. King-Smith and D. Vanderbilt, *Phys. Rev. B* **47**, 1651 (1993); D. Vanderbilt and R. D. King-Smith, *ibid.* **48**, 4442 (1993).
- ¹⁵ Gotthard Saghi-Szabo, Ronald E. Cohen and Henry Krakauer, *Phys. Rev. Lett.* **80**, 4321 (1998).